Diagnostic accuracy of 3D imaging combined with intra-operative ultrasound in the prediction of post-hepatectomy liver failure

Tianchong Wu[1#], Wenhao Huang[2#], Baochun He[3], Yuehua Guo[1], Gongzhe Peng[1], Mingyue Li[1], Shiyun Bao[1]

[1]Department of Hepatobiliary and Pancreatic Surgery, Shenzhen People's Hospital (The Second Clinical Medical College, Jinan University; The First Affiliated Hospital, Southern University of Science and Technology), Shenzhen, China; [2]The Second Clinical Medical College, Jinan University (Shenzhen People's Hospital), Shenzhen, China; [3]Research Lab for Medical Imaging and Digital Surgery, Shenzhen Institutes of Advanced Technology, Chinese Academy of Sciences, Shenzhen, China

Contributions: (I) Conception and design: T Wu, S Bao; (II) Administrative support: S Bao; (III) Provision of study materials or patients: S Bao, T Wu, M Li; (IV) Collection and assembly of data: Y Guo, W Huang, G Peng; (V) Data analysis and interpretation: T Wu, W Huang, B He; (VI) Manuscript writing: All authors; (VII) Final approval of manuscript: All authors.

[#]These authors contributed equally to this work.

Correspondence to: Shiyun Bao. Department of Hepatobiliary and Pancreatic Surgery, Shenzhen People's Hospital, Shenzhen 518020, China. Email: drbsy@sina.com.

Background: The risk of post-hepatectomy liver failure (PHLF) is difficult to predict preoperatively. Accurate preoperative assessment of residual liver volume is critical in PHLF. Three-dimensional (3D) imaging and intra-operative ultrasound (IOUS) offer significant advantages in calculating liver volume and have been widely used in hepatectomy risk assessment. Our research aimed to explore the accuracy of 3D imaging technique combining IOUS in predicting PHLF after hepatectomy.

Methods: We used a retrospective study design to analyze patients who underwent hepatectomy with 3D imaging combined with IOUS between 2017 and 2020. Utilizing 3D reconstruction, the patient's residual liver volumes (PRLVs) and ratio of PRLV to standard liver volume (SLV) were calculated preoperatively. Hepatectomy were performed and actual hepatectomy volume (AHV) were measured. Consistency between preoperative planned hepatectomy volume (PPHV) and AHV was quantified postoperatively by Bland-Altman analysis. Multiple logistic regression and receiver-operating characteristic (ROC) curves were utilized to discuss the predictive value of PRLV/SLV in PHLF.

Results: Among the 214 included patients, 58 (27.1%) had PHLF. Patients with PHLF had significantly higher residual rates of ICG-R15 (%) (P=0.000) and a lower PRLV/SLV ratio (P=0.000). Bland-Altman analysis showed that PPHV was consistent with AHV (P=0.301). Multivariate analysis confirmed that PRLV/SLV ratio >60% (OR, 0.178; 95% CI: 0.084–0.378; P<0.01) was a protective factor for PHLF. The sensitivity, specificity, positive predictive value (PPV), and negative predictive value (NPV) were 75.8% (95% CI: 64.5.3–87.2%), 66.6% (95% CI: 59.1–74.1%), 45.8%, and 88.1%, respectively. The area under the ROC curve (AUC) was 73.7% (95% CI: 65.7–85.8%) and the diagnostic accuracy of PRLV/SLV for PHLF was moderate (P<0.001). These results were validated in the validation cohort perfectly. The primary cohort included 214 patients with a PHLF rate of 27.1% (n=58, 28 grade B and 13 grade C). The validation cohort included 135 patients with a PHLF rate of 35.6% (n=48, 24 grade B and 11 grade C).

Conclusions: The calculation of PRLV/SLV has predictive value in PHLF and can be exploited as a predictive factor. The 3D imaging technique combined with IOUS may be useful for PHLF risk assessment in hepatectomy patients.

Keywords: 3D imaging technique; post-hepatectomy liver failure (PHLF); intraoperative ultrasound (IOUS); hepatectomy

Introduction

Hepatectomy for primary and secondary hepatic malignancy is considered to be a crucial, safe, and standard treatment. However, it is associated with a considerable mortality rate after hepatectomy, which is caused by post-hepatectomy liver failure (PHLF) (1,2). Therefore, accurate preoperative risk assessment and preoperative screening for patients with PHLF are essential for surgeons. Postoperative liver function can be predicted effectively by accurate residual liver ratio calculation. In particular, the assessment of predicted residual liver volumes (PRLVs) and the ratio of PRLV to standard liver volume (SLV) are crucial to evaluating liver function after hepatectomy as well as the risk of PHLF (3). In the past, there were two main methods to measure liver volume; One method is based on height and weight assessment but ignores individual variability. Another is computed tomography (CT) volumetrics, which can be used to calculate liver volume by manually tracing the liver contours in each section and summing the volumes of all sections. However, preoperative liver function assessment based on CT volumetrics alone does have important limitations. First, manual tracing of the liver contours is a time-consuming process. Second, tumor characteristics such as small tumor size, multiple lesions and liver characteristics make CT volumetry an imaging technique with a large margin of error (4-6). Therefore, there is a pressing need to construct an accurate yet simple calculation method to help surgeons evaluate the liver volume of patients, in order to achieve negative surgical margins and reduce the incidence of PHLF.

During preoperative preparation for hepatectomy, the virtual hepatectomy technology of three-dimensional (3D) simulation software can provide visual and more accurate preoperative planning (3,7). However, there are still some difficulties in applying the preoperative hepatectomy plan to the actual intraoperative situation (7,8). Intraoperative ultrasound (IOUS) is utilized to guide this process, which can provide liver surgeons with intuitive and appropriate liver transection lines and assist in locating the precise cutting point of the target vessels in the liver. Nevertheless, this procedure requires in-depth knowledge and experience of the liver anatomy to detect and identify target vessels in

IOUS images (9). In this study, the authors showed that the 3D imaging technique combined with IOUS is superior to traditional image-guided hepatectomy. Using this model, liver surgeons can more intuitively observe the anatomical structure of the specific abdominal organs and vascular systems of patients, calculate the volume of resection and residue, and evaluate the blood supply and bile drainage of the remnant liver (9,10). Virtual planning surgery can also perform this process.

Assessing the PRLV/SLV ratio is decisive in selecting candidates for hepatectomy. Importantly, the ratio of PRLV/SLV seemed able to classify the risk of PHLF (4), but it is unclear if the PRLV/SLV ratio based on the 3D imaging technique is capable of predicting the risk of PHLF. Furthermore, further research is required to confirm whether the PRLV/SLV ratio calculated by the 3D imaging technique combined with IOUS is sufficiently accurate. Hence, this study aimed to assess the ability of the PRLV/SLV ratio calculated by the 3D imaging technique combined with IOUS to predict PHLF. We present the following article in accordance with the STARD reporting checklist (available at https://jgo.amegroups.com/article/view/10.21037/jgo-22-282/rc).

Methods

Study design

A total of 239 patients who underwent liver resection with 3D imaging combined with intraoperative ultrasound at Shenzhen People's Hospital from January 2017 to November 2020 served as the initial cohort for the study. From this initial cohort, 25 patients were excluded from the analysis: one patient was allergic to iodine, two patients refused preoperative treatment, two patients had invalid boundaries, and 20 patients were considered unresectable due to extrahepatic diseases. Finally, 214 patients were included in this analysis. For validation, consecutive patients were collected again in chronological order with the same inclusion criteria. Patients were excluded if they had an allergy to iodine, refused preoperative treatment, were deemed unresectable due to extrahepatic disease, or did not undergo 3D imaging combined with intraoperative

ultrasound. The final primary cohort and validation cohort consisted of 214 and 135 patients, respectively. All patients enrolled in this retrospective analysis and validation cohort underwent hepatectomy navigated by the 3D imaging technique combined with IOUS. The patients' clinical data were gathered and reported according to the STROCSS cohort study guidelines (11). The study was conducted in accordance with the Declaration of Helsinki (as revised in 2013). The study protocol was approved by the ethics committee of Shenzhen People's Hospital (approval No. 5-2017-094). Individual consent for this retrospective analysis was waived.

Patients with PHLF after hepatectomy were determined according to the consensus definition and severity classification of the International Study Group of Liver Surgery (2). The SLV was calculated according to the following formula: liver volume (cm^2) =706 × body surface area $(BSA)(m^2)$ + 2.4, which is a more accurate and unbiased method for estimating total liver volume (TLV), and has been verified in a previous study (1). The ratio of PRLV to SLV was estimated according to the following formula: PRLV/SLV. The BSA was calculated according to the following formula: BSA (m^2) = [body weight (kg) × body height (cm) ÷ 3600]$^{0.5}$ (4).

Surgical planning and resected liver volume prediction

During preoperative preparation, 1.5 mm-thick slice contrast-enhanced CT images were available on a multidetector row CT (Toshiba, Tokyo, Japan, Aquillion 64). The anatomy of the liver, portal vein, and hepatic vein was reconstructed using 3D simulation software (Smart Vision Works; Shenzhen, China). The 3D anatomical structure model of the liver could be reconstructed in 3D simulation software, including the blood supply of the portal vein, the direction of the hepatic vein, the distribution of the biliary tract, the spatial distribution of the hepatic artery variation, as well as the tumor location and its adjacent structure. Based on the Couinaud's anatomical segment theory, the 3D simulation software can calculate the volume of each liver segment and simultaneously perform virtual surgery for hepatectomy. Finally, the PRLV was accurately calculated. Our team totally evaluated the accuracy of the 3D reconstruction software in calculating liver segmentation and PRLV.

During preoperative planning, the reconstructed 3D model image of the hepatectomy cross-section was combined on the 2D CT images, and the cut-off points of both the portal vein and hepatic vein were simultaneously displayed. The authors practiced the procedure simulation using the 3D reconstruction software, and a surgical plan to guide the actual operation was finally determined after discussion by the research team. The position of the IOUS probe can be determined as the initial point in the actual operating field by using IOUS to find the view with the same spatial position as the 2D CT image. The IOUS image findings corresponding to 3D images are immediately displayed in the hepatectomy surface of the actual operation, which allows the detection of IOUS images corresponding to 3D images to be immediately displayed on the surface of the actual liver resection.

During hepatectomy, the extent and margins of hepatectomy were identified in real-time using IOUS. The resection plane was marked intra-operatively. The boundary between the preoperative 3D planned hepatectomy area and the remaining liver area was defined as the real-time interface of hepatectomy. The pringer maneuver was used to dissect the liver parenchyma. The plane of hepatectomy was accurately determined under 3D imaging and IOUS guidance.

Comparison between AHV and PPHV

Accurate PPHV was calculated by virtual planning surgery in the 3D simulation software. The traditional drainage method was used to measure the actual hepatectomy volume (AHV) (3). The excised part of liver was placed into a counting cup that was filled with water, and the volume of spill over water was exactly equal to the AHV. Assessing the consistency between AHV and PPHV can indirectly evaluate the accuracy of obtaining AHV using the 3D imaging guidance of IOUS. The absolute error (AE) and absolute percentage error (PE) were used to evaluate the accuracy of 3D images for IOUS guidance in AHV. The following formulae were applied:

$$AE = \left| PPHV - AHV \right| \qquad [1]$$

$$PE = \frac{AE}{AHV} \qquad [2]$$

Statistical analysis

Statistical analysis was performed using SPSS 22.0 software for Windows (SPSS Inc., Chicago, IL, USA). Continuous data were displayed using the mean ± standard deviation (SD), and were evaluated by *t*-test or the Mann-Whitney U test based on the distribution. Meanwhile, categorical

variables were represented by the n (%), and were assessed using the *Chi-square* test or Fisher's exact test. Related factors of predicting PHLF were analyzed by multiple logistic regression. Bland-Altman analysis (Bland and Altman, 1986) was used to quantify the agreement between PPHV and AHV. A receiver-operating characteristic (ROC) curve was utilized to discuss the predictive value of PRLV/SLV in PHLF. Two-sided P<0.05 was considered statistically significant.

Results

Participants

The primary cohort in this study included 214 consecutive patients, in whom the PHLF rate was 27.1% (n=58, 28 grade B and 13 grade C) according to International Study Group of Liver Surgery (ISGLS) criteria. The validation cohort included 135 consecutive patients with a PHLF rate of 35.6% (n=48, 24 grade B and 11 grade C). *Table 1*

Table 1 Clinical characteristics of hepatectomy patients in the primary study and validation cohorts

Variable	Study cohort (n=214)	Validation cohort (n=135)	P value
Gender (female/male)	33/181	25/110	0.449
Age (y)	57.8±8.3	58.5±9.1	0.471
BMI (kg/m^2)	22.0±2.4	22.2±2.8	0.441
Etiology of hepatectomy			0.374
Benign	8 (3.7)	2 (1.5)	
Primary hepatic carcinoma	195 (91.1)	128 (94.8)	
Metastasis	11 (5.1)	5 (3.7)	
ASA			
I	208 (97.2)	127 (94.1)	0.517
II	6 (2.8)	8 (5.9)	
Background liver disease			
HBV	208 (97.2)	133 (98.5)	0.255
HCV	4 (1.9)	2 (1.5)	0.135
Alcoholic liver cirrhosis	2 (0.9)	0 (0.0)	0.183
Preoperative TACE	10 (4.7)	5 (3.7)	0.664
Laboratory data			
HGB (g/dL)	11.9±1.5	11.8±1.8	0.824
Platelet count (10^9/L)	177.3±112.0	173.1±107.6	0.727
TB (µmol/L)	22.8±15.2	22.7±14.2	0.338
DB (µmol/L)	12.8±9.3	12.5±8.0	0.217
ALT (U/L)	46.8±34.0	43.0±21.0	0.199
AST (U/L)	45.6±29.6	46.5±31.3	0.784
ALB (g/L)	38.4±5.1	37.8±4.8	0.262
INR	0.98±0.18	1.01±0.17	0.200
Liver cirrhosis	174 (81.3)	99 (73.3)	0.079

Table 1 (*continued*)

Table 1 (*continued*)

Variable	Study cohort (n=214)	Validation cohort (n=135)	P value
Liver function status			
Child-Pugh score, median [min–max]	5.0 [5–7]	5.0 [5–8]	0.264
ICG-R15 (%)	7.9±3.9	8.4±4.1	0.230
Tumor diameter (cm)	6.8±2.7	6.4±2.7	0.224
PRLV/SLV (%)	63.2±11.0	63.6±8.3	0.729
Major hepatectomy	117 (54.7)	66 (48.9)	0.292
Open approach	152 (71.0)	101 (74.8)	0.440
Clavien-Dindo classification			
Mild-moderate (grade I–II)	56 (26.2)	44 (32.6)	0.196
Severe (grade III–V)	19 (8.9)	14 (10.4)	0.643
Post-hepatectomy liver failure (%)	58 (27.1)	48 (35.6)	0.094
Grade A	17 (7.9)	13 (9.6)	0.584
Grade B	28 (13.1)	24 (17.8)	0.230
Grade C	13 (6.1)	11 (8.1)	0.456
Postoperative mortality	2 (0.9)	1 (0.7)	0.847

Data are indicated n (%), median [IQR] or $\bar{x}$±s. According to the IHPBA Brisbane 2000 nomenclature, the type of hepatectomy was defined as major and minor resections (≤2 segments: minor; >2 segments: major). BMI, body mass index; ASA, American Society of anesthesiologists; HBV, hepatitis B virus; HCV, hepatitis C virus; TACE, transcatheter arterial chemoembolization; HGB, hemoglobin; TB, total bilirubin; DB, direct bilirubin; ALT, alanine aminotransferase; AST, aspartate aminotransferase; ALB, albumin; INR, international normalized ratio; PRLV, predicted residual liver volumes; SLV, standard liver volume.

displays patient characteristics for the primary and validation cohorts. The prevalence of PHLF between the two cohorts was not statistically significant, and the clinicopathological features of the study and validation cohorts were comparable. As shown in *Table 2*, there were significant differences in the liver function status between PHLF and NPHLF cases in the study cohort.

Accuracy and correlational analysis of PPHV and AHV

Table 3 lists the statistical characteristics of AHV, PPHV, AE, and PE. The average AE and PE were 30.3 cm³ and 8.8%, respectively; the average AHV was 359.3±91.5 cm³; and the average PPHV was 366.3±100.2 cm³ (the average AE and PE were 30.3 cm³ and 8.8%, respectively).

We observed excellent consistency between PPHV and AHV, which was statistically significant (P<0.001). The Bland-Altman plots evaluating the consistency between AHV and PPHV are shown in *Figure 1* (P=0.301), and the

liver volume comparison summary is shown in *Table 3*.

Prediction model development and evaluation

A PRLV/SLV ratio ≥60% (OR, 0.178; 95% CI: 0.084–0.378; P<0.01) was found to be a protective factor against PHLF compared to a PRLV/SLV ratio <60%. On the other hand, ICG-R15 (%) ≥10 (OR, 6.12; 95% CI: 3.007–12.456; P<0.01) and INR (OR, 2.9; 95% CI: 1.15–6.51; P=0.008) were identified as independent risk factors for PHLF by univariate and multivariate analyses. The detailed comparison is shown in *Table 4*.

The ROC curve for PRLV/SLV ratio is shown in *Figure 2*, with an AUC of 0.737 (P<0.001). The ideal cutoff point was calculated as 60%. At the same time, the specificity, sensitivity, negative predictive value (NPV), and positive predictive value (PPV) were 66.6% (95% CI: 59.1–74.1%), 75.8% (95% CI: 64.5.3–87.2%), 88.1%, and 45.8%, respectively.

Table 2 Comparison of the clinicopathological variables between the groups with or without PHLF after hepatectomy

Variable	PHLF (n=58)	NPHLF (n=156)	P value
Gender (female/male)	7/51	26/130	0.408
Age (y)	57.0±11.2	59.0±8.1	0.205
BMI (kg/m^2)	22.4±2.8	22.2±2.8	0.643
Etiology of hepatectomy			0.128
Benign	4 (6.9)	4 (2.6)	
Primary hepatic carcinoma	53 (91.4)	142 (91.0)	
Metastasis	1 (1.7)	10 (6.4)	
ASA			
I	56 (96.6)	152 (97.4)	0.663
II	2 (3.4)	4 (2.6)	
Background liver disease			0.526
HBV	57 (98.3)	151 (96.8)	
HCV	1 (1.7)	3 (1.9)	
Alcoholic liver cirrhosis	0 (0.0)	2 (1.3)	
Laboratory data			
HGB (g/L)	115.1±17.2	120.8±13.9	0.027
Platelet count (10^9/L)	180.7±125.1	176.0±107.1	0.787
TB (µmol/L)	19.9±14.5	23.9±15.4	0.089
DB (µmol/L)	11.3±9.5	13.4±9.2	0.144
ALT (U/L)	38.6±19.4	49.8±37.6	0.005
AST (U/L)	43.6±24.0	46.4±31.4	0.536
ALB (g/L)	38.5±4.8	38.4±5.3	0.869
INR	0.94±0.15	1.00±0.19	0.021
Liver cirrhosis	49 (84.5)	125 (80.1)	0.468
Status of liver function			
Child-Pugh score, median [min–max]	5.0 [5–7]	5.0 [5–7]	0.927
ICG-R15 (%)	10.3±3.4	7.0±3.7	0.000
Tumor diameter (cm)	8.1±3.0	6.3±2.5	0.000
PRLV/SLV (%)	57.4±10.5	65.4±10.3	0.000
Clavien-Dindo classification, n (%)			
Mild-moderate (grade I–II)	29 (50.0)	27 (17.3)	0.000
Severe (grade III–V)	17 (29.3)	2 (1.3)	0.000
Preoperative TACE	6 (10.3)	4 (2.6)	0.026
Operative time (min)	314.3±70.1	286.8±75.5	0.017
Blood loss (mL)	265.5±158.4	244.2±150.4	0.365
Postoperative hospital stay (day)	14.3±2.8	7.1±1.4	0.000

Data are indicated n (%), median [IQR] or $\bar{x}$±s. PHLF, post-hepatectomy liver failure; NPHLF, non post-hepatectomy liver failure; BMI, body mass index; ASA, American Society of anesthesiologists; HBV, hepatitis B virus; HCV, hepatitis C virus; TACE, transcatheter arterial chemoembolization; HGB, hemoglobin; TB, total bilirubin; DB, direct bilirubin; ALT, alanine aminotransferase; AST, aspartate aminotransferase; ALB, albumin; INR, international normalized ratio; PRLV, predicted residual liver volumes; SLV, standard liver volume.

1230

Wu et al. Role of 3D imaging combined with IOUS in predicting PHLF

A typical case to illustrate the process

Preoperative clinical parameters

A 67-year-old man presented with a mass liver lesion on physical examination. An enhanced CT scan of the upper abdomen revealed that the lesion was primarily located in the right liver, about 10.1 cm × 8.4 cm in size, and conformed to the imaging features of hepatocellular carcinoma (*Figure 3*). The patient also had hepatitis B. Liver function was assessed using the Child-Pugh score.

Surgical planning

The 3D model data were reconstructed after processing of the original CT data using Smart Vision Works (SVW), and surgical planning and resectability were evaluated in the 3D model. As shown in *Figure 4*, the 3D model suggested that the tumor oppressed the right portal vein, and was mainly located in the V, VII and VIII hepatic segments. On the basis of anatomical hepatectomy principle, right

hemi-hepatectomy was considered an appropriate surgical method. Virtual surgery was then performed on the 3D model; the PRLV was calculated at 389 cm³, and the PRLV/SLV was only 33.7%, which suggested that direct right hemi-hepatectomy was not feasible.

Laparoscopic ligation of the right branch of the portal vein and secondary hepatectomy were applied. During the third week after the first operation, an enhanced CT scan of the upper abdomen and 3D reconstruction were performed again to formulate the secondary surgical plan. The PRLV was increased significantly to 678 cm³, and the PRLV/SLV reached 58.7%, indicating that right hemi-hepatectomy was safe and feasible (*Figure 5*). The patient underwent secondary surgery and successfully completed laparoscopic right hemi-hepatectomy and right caudate lobe resection based on the preoperative 3D surgical planning and IOUS navigation (*Figure 6*).

Discussion

PHLF is a potentially fatal complication of hepatectomy (12). Most patients with hepatocellular carcinoma are accompanied with chronic liver disease, which is the principal risk factor for PHLF after hepatectomy. Rahbari *et al.* (2) demonstrated a significant correlation between ISGLS's definition of PHLF and perioperative mortality; that is, the probability of perioperative deterioration in grade A, B, and C PHLF patients is 2%, 20%, and 44%, respectively. In grade A patients, it is abnormal in laboratory examination, but routine clinical management treatment can be maintained.

Table 3 Outcomes of AHV and PPHV in the primary study cohort

Variable	Mean	Standard deviation
AHV (cm³)	359.3	91.5
PPHV (cm³)	366.3	100.2
AE (cm³)	30.3	15.0
PE (%)	8.8	4.9

AHV, actual hepatectomy volume; PPHV, preoperative planned hepatectomy volume; AE, absolute error; PE, percentage error.
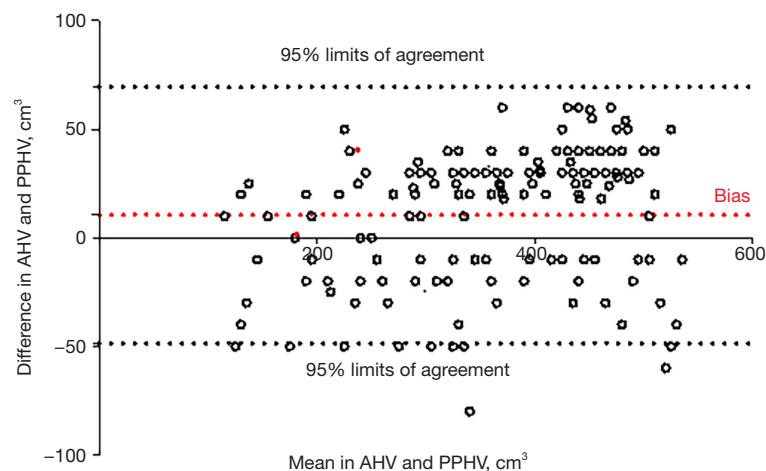
Figure 1 Bland-Altman plots for consistency between AHV and PPHV. AHV, actual hepatectomy volume; PPHV, preoperative planned hepatectomy volume.

**Table 4** Univariate and multivariate logistic regression of PHLF in the primary cohort

Variable	Univariate logistic regression		Multivariate logistic regression	
	OR (95% CI)	P value	OR (95% CI)	P value
HGB (g/dL)				
≥100	1 (reference)	>0.99		
<100	2.8 (1.4–4.3)	0.43	NA	NA
Platelet count (10^9/L)				
>100	1 (reference)	>0.99		
100–50	0.8 (0.4–4.7)	0.74	NA	NA
<50	1.1 (0.5–3.9)	0.56	NA	NA
ALT (U/L)				
>80	1 (reference)	>0.99		
40–80	2.1 (1.4–6.7)	0.11	NA	NA
<40	1.1 (0.5–3.7)	0.23	NA	NA
INR	0.053 (0.006–0.506)	0.011	2.9 (1.15–6.51)	0.008
Tumor diameter (cm)				
>10	1 (reference)			
5–10	1.7 (0.2–6.7)	0.19	NA	NA
<5	1.1 (0.5–3.7)	0.16	NA	NA
PRLV/SLV (%)				
≥60	1 (reference)	>0.99	1 (reference)	>0.99
<60	0.191 (0.092–0.398)	<0.01	0.178 (0.084–0.378)	<0.01
ICG-R15 (%)				
≥10	1 (reference)	>0.99	1 (reference)	>0.99
<10	6.12 (3.007–12.456)	<0.01	6.328 (3.049–13.135)	<0.01
Operative time (min)				
≥300	1 (reference)	>0.99		
<300	0.127 (0.007–2.416)	0.72	NA	NA

PHLF, post-hepatectomy liver failure; HGB, hemoglobin; ALT, alanine aminotransferase; INR, international normalized ratio; PRLV, predicted residual liver volumes; SLV, standard liver volume.

Following extended hepatectomy, there is usually a slight increase in bilirubin or INR, but there is no injury to the patient. Therefore, we defined grades B and C PHLF as "liver failure", as they can lead to a deviation from the conventional clinical treatment. Some authors even believe that class C PHLF should be defined as "liver insufficiency" (1,13-15). In our study cohort, 58 of 214 patients (27.1%) met the ISGLS-PHLF criteria. However, only 13 cases required a change in the clinical management (grade C).

A key factor limiting the implementation of extended hepatectomy is the fact that the future remnant liver (FLR) cannot meet the needs of normal liver function (16). Different strategies, such as ALPPS, portal vein ligation, and portal vein embolization, have been employed to completely remove the liver tumor in cases of small residual liver in the preoperative evaluation (17,18). Inadequate PRLV is a contraindication for hepatectomy and is associated with poor surgery (19). Incorporating the preoperative analysis of

1232

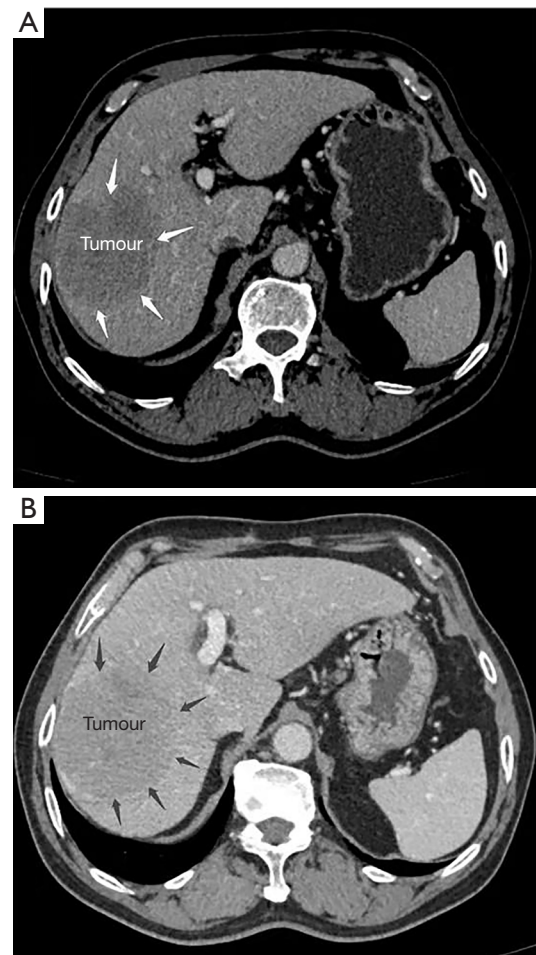Wu et al. Role of 3D imaging combined with IOUS in predicting PHLF
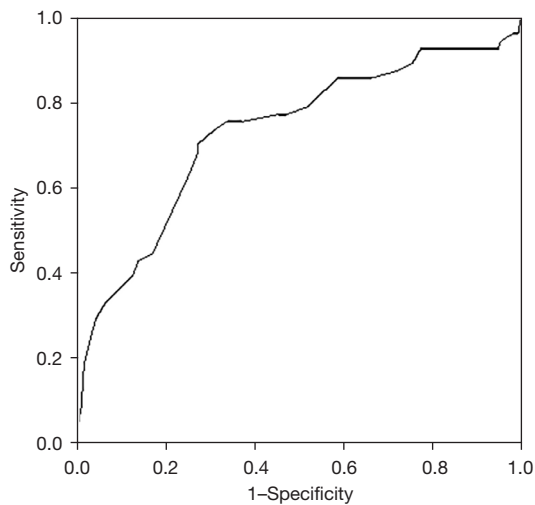
Figure 2 The PRLV/SLV ratio as a predictive factor, as assessed by the ROC curve (AUC 0.737). PRLV, predicted residual liver volumes; SLV, standard liver volume; ROC, receiver-operating characteristic; AUC, area under the curve.


Figure 3 CT scan of the upper abdomen revealed the lesion to be located primarily in the right liver, about 10.1 cm × 8.4 cm in size, and consistent with the imaging features of the hepatocellular carcinoma. (A) Arterial phase; (B) portal venous phase. The arrows indicate the boundary of tumour.

PRLV into the surgical plan of hepatectomy can minimize the risk of PHLF (20). It is known that the most credible determinant of liver dysfunction after subtotal hepatectomy is the patient's residual liver volumes (19,21).

During preoperative preparation for hepatectomy, accurate calculation of the resected and residual liver volumes is essential, which can maximize the risk of postoperative liver failure (7,8). A certain volume of residual liver, adequate blood supply, and biliary drainage are prerequisites for ensuring the safety of the procedure (22). Combined with the planning platform developed in this study, surgeons can easily obtain this information in the best way, because surgeons usually undertake the main task of reconstructing 3D images. With the hepatectomy plane tool provided by SVW, surgeons can manually map the edge of the hepatectomy and make individual surgical plans. Numerous studies have shown that 3D reconstruction software can achieve high efficiency and accuracy in liver volume evaluation (3,5,7,8). Surgeons use these software programs to perform virtual operations before hepatectomy, so as to achieve accurate liver segmentation and calculate the PRLV. At the same time, a number of studies have demonstrated that 3D reconstruction software can accurately measure the PRLV (7,8,10,23,24). Cai *et al.* (3) reported that 3D reconstruction can not only provide a virtual surgical resection plan, but also accurately evaluate the PRLV. Following hepatectomy guidance using the 3D

imaging technique combined with IOUS, the AHV was measured by the drainage method. In our surgical cases, IOUS was used to accurately determine the hepatectomy edge via 3D preoperative planning, which allowed surgeons to clearly understand the surgical resection edge in time and then adjust the surgical resection path in real-time. There was a remarkable consistency between PPHV and AHV (P<0.001). Bland-Altman analysis showed that there was good consistency between the PPHV and AHV (P=0.301). Therefore, it can be assumed that the PPHV using the 3D imaging technique combined with IOUS is coincident to the liver volume of the preoperative targeted resection, and could potentially facilitate precise liver resection. By
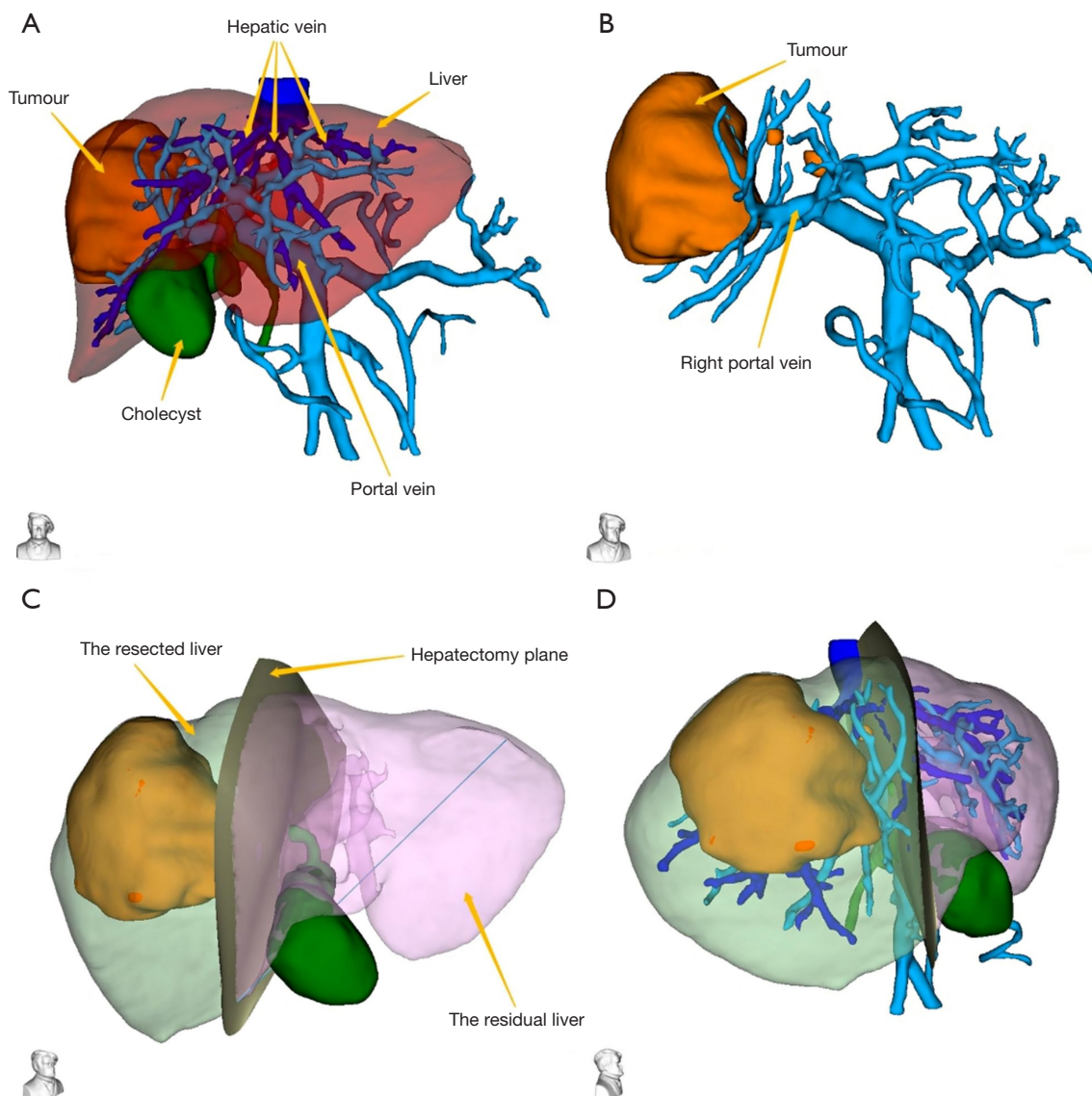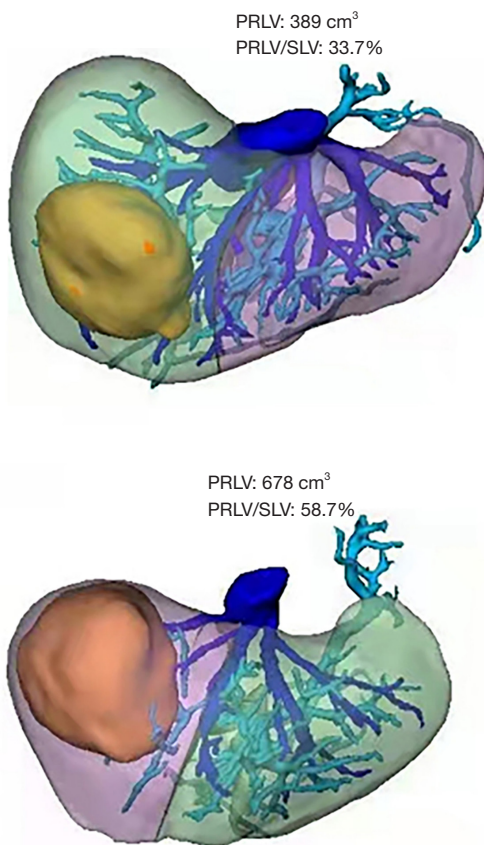
Figure 4 3D model data were reconstructed using Smart Vision Works. (A,B) The tumor oppressed the right portal vein, and was mainly located in the V, VII and VIII hepatic segments; (C,D) the hepatectomy plane was marked in the 3D model.

estimating the statistical relationship between the PPHV and AHV, the accuracy of IOUS in AHV was evaluated (*Table 4*).

In most centers, for patients with different types of hepatectomy, the requirements of the FLR after hepatectomy vary between different types of patients (2,19,25). For patients without underlying parenchymal disease, 25% of the FLR is considered adequate. However, for patients with impaired liver function, at least 40% FLR volume is considered feasible (2,26). Our study demonstrates

the importance of the FLR for postoperative outcomes, which is consistent with previous studies (22,25). Insufficient FLR volume leads to an increase in the incidence of major complications, including postoperative liver failure, deviation from routine clinical treatment, and prolonged hospitalization. For preoperative planning based on 3D reconstruction techniques, the PRLV/SLV ratio is typically used to evaluate the FLR. In the past, the actual TLV was calculated using CT images, but the TLV error calculated using this method was extremely heavy due to the irregular

1234

Wu et al. Role of 3D imaging combined with IOUS in predicting PHLF

PRLV: 389 cm^3
PRLV/SLV: 33.7%

PRLV: 678 cm^3
PRLV/SLV: 58.7%

Figure 5 Virtual surgery was performed on the 3D model, and the PRLV and PRLV/SLV were calculated before and after laparoscopic ligation of the right branch of the portal vein. PRLV, predicted residual liver volumes; SLV, standard liver volume.

Figure 6 Laparoscopic right hemi-hepatectomy and right caudate lobe resection based on the preoperative 3D surgical planning and IOUS navigation. IOUS, intraoperative ultrasound.

shape of the tumor and the appearance of satellite lesions (1,3,7,27). In our study, SLV was used to estimate the actual TLV since SLV was estimated based on body surface area, which was not affected by potential liver disease and was more closely related to a healthy liver. Fitting into the PRLV/SLV ratio instead of the PRLV/TLV ratio actually raised the standard of surgery, because the TLV would be reduced due to other hepatic diseases such as liver cirrhosis. We hypothesized that the rate of PHLF depends on the PRLV/SLV ratio in hepatectomy patients. The PRLV/SLV ratio decrease in hepatectomy patients is more likely to be related to PHLF. In our patients, the AUC of the PRLV/SLV ratio was 73.7%, with a 95% CI: 65.7–85.8 (P<0.001). Also, PHLF was more likely occur in cases with preoperative PRLV/SLV ratios ≤60%, and the sensitivity, specificity, PPV, and NPV of the PRLV/SLV ratio for predicting PHLF were 75.8% (95% CI: 64.5.3–87.2), 66.6% (95% CI: 59.1–74.1), 45.8%, and 88.1%, respectively. These findings were substantiated using the validation cohort.

In our study, multivariate analysis showed that the ICG-R15 (%) clearance test and INR were independent risk factors for PHLF. However, despite the fact that the ICG-R15 (%) clearance test was the first method to introduce quantitative liver testing, its effect on PHLF remains controversial (1,28,29). Previous studies have found that ICG-R15 (%) clearance test can be widely used in liver surgery, but its application in preoperative liver function assessment is only reliable in selected groups of patients with liver cirrhosis, which limits its universal application (1,30,31). To master this knowledge, hepatobiliary surgeons should focus on novel strategies, so as to overcome the shortcomings of the old methods.

There are still some limitations in this study that should be noted. Firstly, this was a retrospective study. Secondly, the small number of included cases imposes restrictions on our statistical analysis. Our findings would be more compelling if PRLV/SLV were validated in another validation set and compared with other established models. Based on 3D imaging technology and IOUS, the clinical application value of PRLV/SLV will be further explored in future prospective studies.

Conclusions

Liver function reflects a series of metabolic functions, which cannot be measured simultaneously by any single detection

method. The calculation of PRLV/SLV has predictive value in PHLF and can be exploited as a predictive factor. The 3D imaging technique combined with intra-operative ultrasound may be useful for PHLF risk assessment in hepatectomy patients.

Acknowledgments

Footnote

Reporting Checklist: The authors have completed the STARD reporting checklist. Available at https://jgo.amegroups.com/article/view/10.21037/jgo-22-282/rc

Data Sharing Statement: Available at https://jgo.amegroups.com/article/view/10.21037/jgo-22-282/dss

Conflicts of Interest: All authors have completed the ICMJE uniform disclosure form (available at https://jgo.amegroups.com/article/view/10.21037/jgo-22-282/coif). All authors report the technical and equipment assistance in data collection and analysis from the imaging center of Shenzhen Yitu Intelligent Technology Co., Ltd. The authors have no other conflicts of interest to declare.

Ethical Statement: The authors are accountable for all aspects of the work in ensuring that questions related to the accuracy or integrity of any part of the work are appropriately investigated and resolved. The study was conducted in accordance with the Declaration of Helsinki (as revised in 2013). The study protocol was approved by the ethics committee of Shenzhen People's Hospital (approval No. 5-2017-094). Individual consent for this retrospective analysis was waived.

References

1. Navarro JG, Yang SJ, Kang I, et al. What are the most important predictive factors for clinically relevant posthepatectomy liver failure after right hepatectomy for hepatocellular carcinoma? Ann Surg Treat Res 2020;98:62-71.

2. Rahbari NN, Garden OJ, Padbury R, et al. Posthepatectomy liver failure: a definition and grading by the International Study Group of Liver Surgery (ISGLS). Surgery 2011;149:713-24.

3. Cai W, Fan Y, Hu H, et al. Postoperative liver volume was accurately predicted by a medical image three dimensional visualization system in hepatectomy for liver cancer. Surg Oncol 2017;26:188-94.

4. Cieslak KP, Runge JH, Heger M, et al. New perspectives in the assessment of future remnant liver. Dig Surg 2014;31:255-68.

5. Kubota K, Makuuchi M, Kusaka K, et al. Measurement of liver volume and hepatic functional reserve as a guide to decision-making in resectional surgery for hepatic tumors. Hepatology 1997;26:1176-81.

6. Vauthey JN, Chaoui A, Do KA, et al. Standardized measurement of the future liver remnant prior to extended liver resection: methodology and clinical associations. Surgery 2000;127:512-9.

7. Yang J, Tao HS, Cai W, et al. Accuracy of actual resected liver volume in anatomical liver resections guided by 3-dimensional parenchymal staining using fusion indocyanine green fluorescence imaging. J Surg Oncol 2018;118:1081-7.

8. Fang CH, Tao HS, Yang J, et al. Impact of three-dimensional reconstruction technique in the operation planning of centrally located hepatocellular carcinoma. J Am Coll Surg 2015;220:28-37.

9. D'Hondt M, Vandenbroucke-Menu F, Préville-Ratelle S, et al. Is intra-operative ultrasound still useful for the detection of a hepatic tumour in the era of modern pre-operative imaging? HPB (Oxford) 2011;13:665-9.

10. Takamoto T, Mise Y, Satou S, et al. Feasibility of Intraoperative Navigation for Liver Resection Using

Real-time Virtual Sonography With Novel Automatic Registration System. World J Surg 2018;42:841-8.

11. Agha RA, Borrelli MR, Vella-Baldacchino M, et al. A protocol for the development of the STROCSS guideline: Strengthening the Reporting of Cohort Studies in Surgery. Int J Surg Protoc 2017;5:15-7.

12. Liu JY, Ellis RJ, Hu QL, et al. Post Hepatectomy Liver Failure Risk Calculator for Preoperative and Early Postoperative Period Following Major Hepatectomy. Ann Surg Oncol 2020;27:2868-76.

13. van den Broek MA, Olde Damink SW, Dejong CH, et al. Liver failure after partial hepatic resection: definition, pathophysiology, risk factors and treatment. Liver Int 2008;28:767-80.

14. Lin XJ, Yang J, Chen XB, et al. The critical value of remnant liver volume-to-body weight ratio to estimate posthepatectomy liver failure in cirrhotic patients. J Surg Res 2014;188:489-95.

15. Manizate F, Hiotis SP, Labow D, et al. Liver functional reserve estimation: state of the art and relevance for local treatments: the Western perspective. J Hepatobiliary Pancreat Sci 2010;17:385-8.

16. Allen PJ, Jarnagin WR. Current status of hepatic resection. Adv Surg 2003;37:29-49.

17. Olthof PB, Huiskens J, Wicherts DA, et al. Survival after associating liver partition and portal vein ligation for staged hepatectomy (ALPPS) for advanced colorectal liver metastases: A case-matched comparison with palliative systemic therapy. Surgery 2017;161:909-19.

18. Schadde E, Ardiles V, Robles-Campos R, et al. Early survival and safety of ALPPS: first report of the International ALPPS Registry. Ann Surg 2014;260:829-36; discussion 836-8.

19. Schindl MJ, Redhead DN, Fearon KC, et al. The value of residual liver volume as a predictor of hepatic dysfunction and infection after major liver resection. Gut 2005;54:289-96.

20. Mayer P, Grözinger M, Mokry T, et al. Semi-automated computed tomography Volumetry can predict hemihepatectomy specimens' volumes in patients with hepatic malignancy. BMC Med Imaging 2019;19:20.

21. Pulitano C, Crawford M, Joseph D, et al. Preoperative assessment of postoperative liver function: the importance of residual liver volume. J Surg Oncol 2014;110:445-50.

22. Lock JF, Malinowski M, Seehofer D, et al. Function and volume recovery after partial hepatectomy: influence of preoperative liver function, residual liver volume, and obesity. Langenbecks Arch Surg 2012;397:1297-304.

23. Fang CH, Liu J, Fan YF, et al. Outcomes of hepatectomy for hepatolithiasis based on 3-dimensional reconstruction technique. J Am Coll Surg 2013;217:280-8.

24. Cai W, He B, Fan Y, et al. Comparison of liver volumetry on contrast-enhanced CT images: one semiautomatic and two automatic approaches. J Appl Clin Med Phys 2016;17:118-27.

25. Zhang Z, Ouyang G, Wang P, et al. Safe standard remnant liver volume after hepatectomy in HCC patients in different stages of hepatic fibrosis. BMC Surg 2021;21:57.

26. Ribero D, Amisano M, Bertuzzo F, et al. Measured versus estimated total liver volume to preoperatively assess the adequacy of the future liver remnant: which method should we use? Ann Surg 2013;258:801-6; discussion 806-7.

27. Chun YS, Ribero D, Abdalla EK, et al. Comparison of two methods of future liver remnant volume measurement. J Gastrointest Surg 2008;12:123-8.

28. Luo Y, Zhang Y, Yang L, et al. Value of continuous monitoring of ICG-R15 in assessing hepatic insufficiency after partial hepatectomy. Journal of Clinical Hepatology 2018;34:1055-9.

29. Kure S, Kaneko T, Takeda S, et al. The feasibility of Makuuchi criterion for resection of hepatocellular carcinoma. Hepatogastroenterology 2007;54:234-7.

30. Wang YY, Zhao XH, Ma L, et al. Comparison of the ability of Child-Pugh score, MELD score, and ICG-R15 to assess preoperative hepatic functional reserve in patients with hepatocellular carcinoma. J Surg Oncol 2018;118:440-5.

31. Tralhao JG, Hoti E, Oliveiros B, et al. Study of perioperative liver function by dynamic monitoring of ICG-clearance. Hepatogastroenterology 2012;59:1179-83.